第 51 卷第 2 期 中国科学技术大学学报 Vol. 51, No. 2
2021 年 2 月 JOURNAL OF UNIVERSITY OF SCIENCE AND TECHNOLOGY OF CHINA Feb. 2021
Received: 2021-02-06; Revised: 2021-02-22 doi:10.52396/JUST-2021-0045

Three-dimensional array materials for electrocatalytic water splitting

LIU Qilong[1], XIAO Chong[1,2]*
1. Institute of Energy, Hefei Comprehensive National Science Center, Hefei 230031, China;
2. Hefei National Laboratory for Physical Sciences at the Microscale, Hefei 230026, China
* Corresponding author. E-mail: cxiao@ustc.edu.cn

Abstract: Hydrogen energy is considered to be one of the clean energy sources most likely to alternate fossil fuels. The exploration of catalytic materials suitable for electrocatalytic water splitting to produce hydrogen has become an important subject in the field of water electrolysis. Limited to the phenomena of easy stacking of nano-powder materials and poor conductivity during the catalytic reaction, the combination of nano-active materials and conductive substrates to construct three-dimensional (3D) array electrodes with open porous structures has become a research hotspot. This article first summarizes the advantages of 3D array electrodes for water electrolysis, then briefly describes several strategies for improving the catalytic performance of materials, and finally classifies and summarizes the array catalytic materials used for water electrolysis. It is expected to provide reference for the design and synthesis of electrocatalytic materials in the future.

Keywords: electrocatalytic water splitting; hydrogen energy; 3D array electrode
CLC number: TQ426 **Document code**: A

1 Introduction

The exploitation and utilization of fossil fuels has greatly promoted the development of human society, but its excessive use releases tremendous harmful substances and carbon dioxide, which has caused the environmental pollution and greenhouse effect[1,2]. Carbon dioxide emissions in China are supposed to reach the peak by 2030 and achieve the carbon neutrality by 2060. Some measures to reduce the use of fossil fuels are imperative.

When hydrogen is burned, it gives off a lot of heat, and only water is produced. It is considered to be one of the new energy sources most likely to replace fossil fuels[3,4]. As early as the end of the 18th century, Troostwijk and Deiman et al. discovered that water electrolysis can produce hydrogen and oxygen[5]. Cavendish later confirmed this phenomenon and proved that the volume of H_2 is twice that of O_2[6]. With the advancement of science and technology, the technology of hydrogen production from electrolysis of water will gradually satisfy people's demand for hydrogen energy.

Hydrogen production by electrolysis of water can be simply written as Equation(1) (Figure 1):

$$2H_2O \rightarrow 2H_2 + O_2 \quad (1)$$

Under standard conditions, 237.1 kJ·mol^{-1} energy is required to drive the water dissociation reaction,

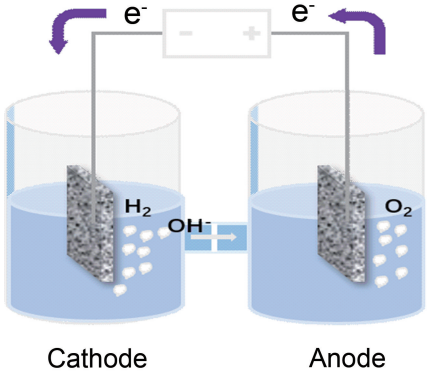

Figure 1. Schematic diagram of water electrolysis device.

which corresponds to the 1.23 V voltage requirement in thermodynamics[7]. Electrocatalytic water splitting includes an oxygen evolution reaction (OER) that generates oxygen on the anode and a hydrogen evolution reaction (HER) that generates hydrogen on the cathode[8,9]. The overpotential required in the electrocatalytic water splitting not only has to cross the inherent activation barriers of the cathode and anode, but also needs to overcome the potentials caused by other resistances, such as contact resistance and solution resistance[10]. The potential contact resistance and solution resistance are unavoidable[11,12]. Scientists have

Citation: LIU Qilong, XIAO Chong. Three-dimensional array materials for electrocatalytic water splitting. J. Univ. Sci. Tech. China, 2021, 51(2): 87-102.

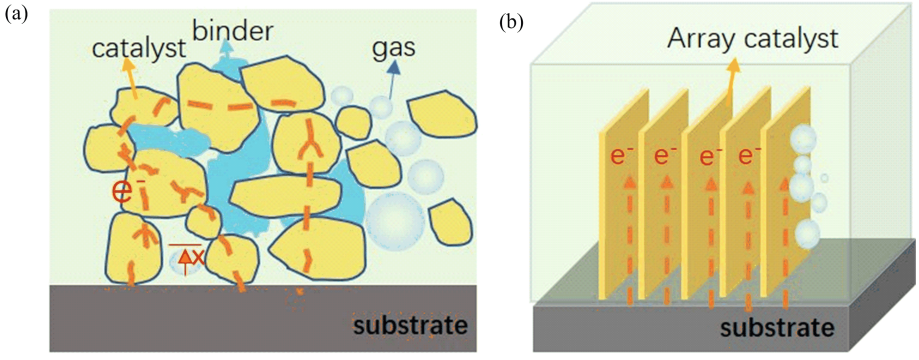

Figure 2. Schematic diagrams of different working electrodes. (a) the membrane electrode coated with nano-powder material. (b) 3D array electrode.

been working hard to explore new types of catalytic materials to reduce the activation barrier of the cathode or anode and reduce the over-potential required in the catalytic process.

In the process of exploring electrocatalytic materials, it was found that the more active sites exposed by the catalyst material and the lower the charge transfer resistance, the smaller the overpotential required in the electrocatalytic process[13]. Larger-sized powder materials tend to aggregate, are not conducive to contact with catalytic reaction species, and have insufficient conductivity, so they are generally not suitable for the direct use as electrochemical catalysts. If the size of the material is reduced to the nanometer size, or even to the atomic size level, a larger number of catalytic sites can be exposed on the catalyst surface, which is conducive to the positive progress of the catalytic reaction[14]. Doping engineering strategies, defect engineering strategies, and morphology adjustment engineering strategies have all been proven to effectively improve the conductivity of the catalyst and accelerate the kinetic process of the catalytic reaction. Although great progress has been made in improving the catalytic performance, nanomaterials still have certain limitations in the catalytic reaction. Generally, the aggregation and accumulation of catalytic materials prevents effective contact between active sites and reactive substances, resulting in a large number of active sites in an idle state, which is not conducive to the progress of the catalytic reaction[15]. Combining nano-active materials with conductive substrate (such as one-dimensional nanowires, two-dimensional nanosheets, three-dimensional nickel foam (NF), and copper foam) to form a 3D array material can effectively reduce the adverse effects of nanoparticle aggregation[16]. 3D materials with hierarchical structures have attracted widespread attention[17]. Compared with nano-powder materials, 3D catalytic materials have a larger specific surface area, which exposes a larger number of catalytic active sites, and the catalytic performance is significantly improved.

Array materials can improve the catalytic performance from the following aspects. (i) The active material is directly connected to the substrate, avoiding the influence of the adhesive and accelerating the electron transfer rate[18]. (ii) The array structure has a larger specific surface area and is exposed to more active sites[19]. (iii) The 3D open structure enables the rapid diffusion of reactive species and timely release of the generated gas, preventing bubbles from accumulating on the surface of the catalyst to affect the catalytic process[20, 21]. The schematic diagrams of the 3D array electrode and the membrane electrode coated with nano-powder is shown in Figure 2. (iv) Appropriate base materials and active materials cooperate to promote the electrocatalytic reaction together[22]. (v) Finally, by optimizing the conditions of the synthesis method, the crystal structure and morphology of the array material can be adjusted to promote the electron transfer rate and accelerate the kinetics of the catalytic reaction[23, 24].

3D Array materials still occupy an important position in the future research of catalysis. This review will briefly describe the principles of electrocatalytic water splitting reactions, various strategies to improve the electrocatalytic performance, and sort out different kinds of catalysts used for electrolytic water splitting recently reported, hoping to provide reference for the design and synthesis of new materials in the future.

2 Reaction mechanism

2.1 HER mechanism

HER involves the transfer process of two electrons[25]. Studies have shown that the hydrogen evolution has two reaction mechanisms, Volmer-Heyrovsky mechanism and Volmer-Tafel mechanism, consisting of Volmer step, Heyrovsky step and Tafel step. In different electrolyte environments, these two reaction mechanisms are also different[26, 27].

In acidic media, H^+ is relatively abundant, so it is easily adsorbed on the active sites on the surface of the catalyst and transformed into an intermediate state.

$$H^+ + e^- \rightarrow H_{ad} \quad \text{Volmer step} \quad (2)$$

This intermediate hydrogen atom is called the adsorbed hydrogen (H_{ad}). This hydrogen adsorption process is called the Volmer step. There are two cases of hydrogen synthesis on the catalyst surface. One is the combination of H_{ad} and free H^+ to release hydrogen.

$$H_{ad} + H^+ + e^- \rightarrow H_2 \quad \text{Heyrovsky step} \quad (3)$$

This process is called the Heyrovsky step. The other is the combination of two H_{ad} to form hydrogen molecules to release.

$$2H_{ad} \rightarrow H_2 \quad \text{Tafel step} \quad (4)$$

This process of combining two adsorbed hydrogens is called the Tafel step.

In alkaline and neutral environments, the hydrogen adsorption and desorption steps are different from those in acidic conditions. Due to insufficient H^+, water molecules produce H^+ by the applied potential, and then adsorb on the materials to produce H_{ad} (Equation (5))[25].

$$H_2O + e^- \rightarrow H_{ad} + OH^- \quad \text{Volmer step} \quad (5)$$

This process of producing H_{ad} is different from the direct adsorption of H^+ in an acidic environment. The following Heyrovsky step and Tafel step are similar to those in an acidic environment, generating hydrogen molecules for the combination of adsorbed hydrogen and hydrogen ions and the combination of two adsorbed hydrogens[28, 29].

$$H_{ad} + H_2O + e^- \rightarrow H_2 + OH^- \quad \text{Heyrovsky step} \quad (6)$$

The Heyrovsky step is the same as the reaction equation(6), and the Tafel step is the same as the reaction equation(4).

Specifically, compared with acidic environments, electrocatalytic processes in alkaline and neutral environments require more energy to drive the dissociation of water. Therefore, it is necessary to comprehensively consider the delicate balance between the energy required for the hydrolysis process and the Gibbs free energy of H adsorption during the designing of HER catalytic materials in an alkaline environment.

2.2 OER mechanism

OER is another important half-reaction of the electrocatalytic water splitting. It has undergone a four-electron transfer process, involving a variety of intermediate conversion processes. The electrocatalysis process requires more energy to overcome the kinetic barrier, so the catalytic material needs a greater driving voltage to generate oxygen in catalysis. The study found that the oxygen generation process in different environments is shown in the following reaction equation, where M indicates the active sites on the catalyst surface[30, 31].

In acid medium:

$$M + H_2O \rightarrow M{-}OH + H^+ + e^- \quad (7)$$

$$M{-}OH \rightarrow M{-}O + H^+ + e^- \quad (8)$$

$$M{-}O + H_2O \rightarrow M{-}OOH + H^+ + e^- \quad (9)$$

$$M{-}OOH \rightarrow M + O_2 + H^+ + e^- \quad (10)$$

In an alkaline environment:

$$M + OH^- \rightarrow M{-}OH + e^- \quad (11)$$

$$M{-}OH + OH^- \rightarrow M{-}O + H_2O + e^- \quad (12)$$

$$M{-}O + OH^- \rightarrow M{-}OOH + e^- \quad (13)$$

$$M{-}OOH + OH^- \rightarrow M + O_2 + H_2O + e^- \quad (14)$$

As the reaction progresses, the reactive species in the electrolyte gradually bond with the active sites to generate intermediate products M−OH, M−O and M−OOH, and finally oxygen. Studies have found that the formation of these intermediate products requires a certain amount of driving energy. The step with the highest energy barrier is called the rate-limiting step of OER, which also directly determines the catalytic efficiency of the material. What is interesting is that the total energy required for the two steps of M−OH→M−O (reaction equations(8) and (12)) and M−O→M−OOH (reaction equations (9) and (13)) is basically the same, no matter under acidic or alkaline conditions, approximately 3.2 eV[32, 33]. Therefore, in the process of designing OER catalytic materials, it is necessary to adjust the adsorption energy of M−O at an appropriate position between M−OH and M−OOH to reduce the change of the Gibbs free energy and achieve the purpose of improving catalytic efficiency.

3 Strategies to improve catalytic performance

With in-depth research on catalytic materials, the mechanism of electrocatalytic water splitting has gradually become clear. More and more strategies have been developed to improve the electrocatalytic activity. The morphology modification strategy, ion doping strategy, manufacturing vacancy strategy and phase change strategy have proved to be effective methods for the improvement of electrocatalytic performance.

3.1 Morphology change strategy

When different catalytic materials have the same composition, the catalytic materials with different morphologies often contain different specific surface areas, so their catalytic performance is also different. For example, the electrocatalytic activity of MnO_2 nanospheres and nanowires is better than that of nanoparticles, because nanospheres and nanowires have a relatively large specific surface area[34]. Qiao et al. also reported that the OER and oxygen reduction reaction (ORR) performance of the Co_3O_4 nanowire

array with a hollow structure is better than the corresponding micro-nano powder materials[35]. Therefore, by adjusting the microscopic morphology of the catalytically active material, a larger number of active sites can be exposed, the catalytic performance of the material can be effectively improved. Recent reports such as Mo-doped Ni_3S_2 with the nanoneedles array[36], metal @ metallic hydroxide nanoarray with the core-shell structure[37] and $CuCo_2O_4$ with the nanosheet array[38] have discussed the influence of morphological changes on the catalytic performance.

3.2 Ion doping strategy

Doping an appropriate number of heteroatoms into the basic catalytic material can adjust the inherent electronic environment around the doped atoms, which is conducive to the positive progress of the reaction. Metal elements Fe, Co, Ni, etc. and non-metal elements N, P, etc. belong to two common doping sources[39-41]. Zhang et al. successfully incorporated Al elements into Ru nanosheets[42]. In the HER test under acidic conditions, a current density of 10 mA · cm^{-2} can be achieved with an overpotential of 79 mV, which is less than the overpotential required for elemental Ru. In addition, catalytic materials prepared with N, P and B as doping sources have also been reported[43-45]. We have used hexamethylenetetramine as the source of N element to study the effect of N doping on the catalytic performance of MoS_2 nanosheets[46]. After the test , it is found that the doped N elements can improve the HER activity of the base material and maintain good stability. These reports indicate that the appropriate incorporation of heteroatoms can effectively improve the conductivity of the base material, activate the inert sites near the doped heteroatoms, and effectively improve the catalytic performance. In addition to single-element doping, catalysts that use multi-element doping strategies to improve catalytic activity have also been studied. For example, Ni_3S_2 nanoflowers co-doped with Fe and Mn are used to enhance the OER activity[47], porous carbon modified with Pt and Er is used to improve the performance of the electrolyzed water[48], and carbon nanotubes co-doped with N and Co are used for Zn-air batteries and the electrolyzed water[49].

3.3 Vacancy manufacturing strategy

Oxygen vacancies are usually used as donors to narrow the band gap, thereby increasing the carrier concentration and conductivity of the material[50]. Because the defect energy level of oxygen vacancies exists under the conduction band, it is conductive to the transfer of valence band electrons to the metal 3D orbital, adjusts the adsorption capacity of the active site to the reaction medium, and fundamentally improving the catalytic efficiency of the matrix[51]. The methods for generating oxygen vacancies in the laboratory include plasma treatment, $NaBH_4$ reduction[52], and lithium-ion reduction[53], etc. Wang et al. used Ar plasma treatment to generate vacancies on the surface of Co_3O_4 nanosheets[54]. Even though the surface of the nanosheet becomes rough after plasma etching, the OER performance is improved by 10 times. This may be the generation of oxygen vacancies exposed to a greater number of active sites. They also used plasma technology to introduce sulfur vacancies in MoS_2[55], change the electronic structure state of the material surface, and enhance the HER catalytic activity of the base material. In addition to these materials, $LaFeO_3$ nanofibers[56], Fe-doped $W_{18}O_{49}$[57], NiO nanosheets[58], etc. processed by the vacancy manufacturing engineering have also been used to explore the electrocatalytic reduction of nitrogen to ammonia.

3.4 Phase change strategy

In the process of exploring catalytic materials, it is found that the phase transition of the material also has a certain influence on its catalytic activity. Compare 2H-MoS_2 with hexagonal symmetry and 1T-MoS_2 with square symmetry. When MoS_2 changing from 2H phase to 1T phase, the external charge changes the density of states near the Fermi surface, which makes 1T-MoS_2 show metallic characteristics[59]. The increase in charge density is conducive to the rapid transfer of electrons in the catalytic process. Voiry performed partial oxidation of different phases of MoS_2 to explore the active sites. According to the research, the active sites of 2H-MoS_2 are mainly distributed in the boundary area, and 1T-MoS_2 with metallic characteristics is not only in the boundary area, but also has many exposed active sites in the plane of the matrix material[60]. Not only MoS_2 materials, Chen et al. reported that when MnO_2 exhibits different phases, their catalytic performance is also different[34].

3.5 Building an array structure strategy

Growing active materials with an array structure in situ on the porous conductive substrate effectively exposes more active sites, avoids the use of binders, and facilitates the rapid transfer of electrons. The ordered array structure can also enable the rapid diffusion of reactive species and timely release of the generated gas, which is conducive to the positive progress of the catalytic reaction. If different strategies to improve the catalytic activity are combined with the strategy for constructing an array structure, the two methods can synergistically increase the catalytic activity. Using Ru to adjust the electronic structure of the NiFe-P nanosheet array, effectively improving the inherent conductivity and catalytic activity of the matrix material[61]. In 1 mol · L^{-1} KOH electrolyte, when Ru-doped NiFe-P

nanosheet array electrodes are used for HER and OER tests, only 44 and 242 mV overpotentials are required to reach a current density of 10 mA · cm^{-2}, respectively. When used in water splitting reaction, only 1.47 V is required, which is better than the performance of noble metal-based catalytic materials. In addition, 3D array structures such as Ni-Fe oxyhydroxide @ NiFe alloy nanowire array with heterogeneous structures[62] and MoS_2/NiS_2 nanosheet arrays rich in defects[63] have also been used to study electrocatalytic water splitting.

4 Electrochemical performance evaluation

The tests of HER and OER in the laboratory are all carried out with a three-electrode system in an electrolyte environment. Generally, the 3D array electrode is directly used as the working electrode, the Ag/AgCl electrode or the saturated calomel electrode is used as the reference electrode, and the carbon rod or Pt sheet electrode is used as the counter electrode. The main idea of the three-electrode test system is to eliminate the ohmic voltage drop between the working electrode and the counter electrode caused by the solution and other factors by introducing the reference electrode, and then truly show the polarization phenomenon of the studied material itself. Tests such as overpotential, electrochemically active surface area (ECSA), Tafel slope, electrochemical impedance spectroscopy (EIS), and stability test are used to demonstrate the catalytic performance of the material.

4.1 Overpotential

Due to the existence of kinetic obstacles, both HER and OER need to apply a certain overpotential to make the reaction proceed. The overpotential is generally obtained by linear scanning voltammetry (LSV). From the perspective of catalysis, the current density of 10 mA · cm^{-2} is equivalent to the approximate current density of approximately 10% of solar-fuel conversion efficiency under sunlight, and is a key measure of electrocatalytic reactions[64]. Therefore, the smaller the overpotential required for the catalyst to reach the current density of 10 mA · cm^{-2}, the better the catalytic performance of the material. Since the 3D array material is easy to reach a larger current density, it is usually compared to the overpotential required to reach a larger current density, such as 50 or 100 mA · cm^{-2}.

4.2 ECSA

ECSA is an important parameter to evaluate the electrocatalytic performance of materials. With the deepening of the exploration of nanomaterials and the gradual increase of the specific surface area, the geometric surface area of the material is not enough to reflect the active area of the material. In the process of cyclic voltammetry (CV), the non-faradaic current density has a linear relationship with the scan rate, so ECSA can be used to reflect the number of active sites on the surface of the material. The larger the electrochemically active surface area, the more active sites the material contains and the better the catalytic performance.

4.3 Tafel slope

The Tafel slope reflects the charge transfer ability in the catalytic process. The smaller the Tafel slope, the stronger the charge transfer ability. The Tafel slope can be obtained by converting the LSV curve data[65], as shown in Equation(15):

$$\eta = a + b \cdot \log |j| \tag{15}$$

Where η, j, a and b represent overpotential, current density, Tafel constant and Tafel slope, respectively. The calculated slope of the linear part is the Tafel slope. It is worth noting that although the material with a lower Tafel slope has a stronger charge transfer ability, the resistance of the catalyst and electrolyte that need to be crossed during charge transfer cannot be ruled out[66]. Therefore, a catalyst with better performance requires a lower Tafel slope, a smaller overpotential, and a larger current density.

4.4 EIS

EIS is used to show the catalytic kinetic performance of the material. The test system is regarded as an equivalent circuit composed of resistance, capacitance and inductance in different ways, and a small amplitude AC voltage or current disturbance is applied to it to obtain AC impedance spectroscopy data. According to EIS to analyze the charge transfer behavior during the catalytic reaction. Generally, the smaller the charge transfer resistance (R_{ct}), the faster the electron transfer rate, which is more conducive to the progress of the catalytic reaction.

4.5 Stability test

Stability or durability is an important indicator of the actual application of the catalyst, showing the ability of the catalyst to maintain its activity for a long time. Stability test is to record the change of current density under constant overpotential. Over a long period of the test, the smaller the change of the current density, the better the stability of the catalyst. It can also be evaluated by continuous CV cycles. If the overpotential before and after LSV is almost unchanged, it means that the material has a good durability.

5 Catalytic material with array structure

In recent years, the electrocatalytic water splitting hydrogen production technology has gradually matured, and the promotion of hydrogen energy has also made certain progress. However, the current catalytic materials used for electrolysis of water are still precious metals[67]. Commercial Pt/C is used in the report to

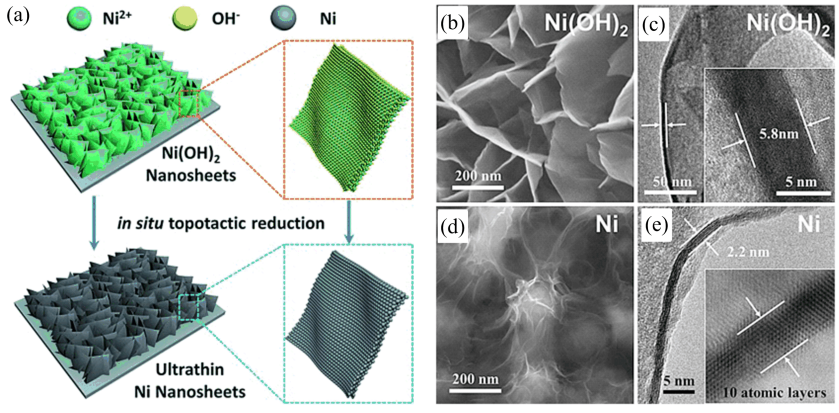

Figure 3. Schematic diagram and characterization of the elemental nickel nanosheet arrays. (a) In-situ topological reduction reaction to generates atomic-thick Ni nanosheet arrays; (b,d) SEM images of $Ni(OH)_2$ array and Ni array; (c,e) HR-TEM images of the curled $Ni(OH)_2$ nanosheets and vertical Ni nanosheets. The inset in the images show the thickness of the $Ni(OH)_2$ and elemental Ni nanosheets, respectively. Reproduced with permission from Ref. [68]. Copyright 2015, John Wiley and Sons.

measure the HER performance of other new catalytic materials, and RuO_2 or IrO_2 is used to measure the OER performance. Some metal compound catalytic materials have received widespread attention due to their suitable electronic structure, easy-to-adjust electrical conductivity, and excellent electrochemical activity and stability. Combining the metal-based material modified by the above strategy with a conductive substrate to form a 3D array electrode could be directly used as the working electrode of HER and OER, which has become a hot spot in recent research on hydrogen production by electrolysis of water.

5.1 Elemental metal or alloy elemental array catalyst

For a single metal array catalyst, Sun et al. first grew ultra-thin $Ni(OH)_2$ nanosheet arrays in situ on the surface of NF, after the in-situ topological reduction step, the elemental Ni material produced by the reduction reaction still maintains the nanosheet array morphology (Figure 3(a))[68]. These Ni nanosheet arrays distributed on the surface of NF can quickly transfer electrons without being delayed by the binder, and the porous structure of NF ensures the rapid diffusion of reactive species and the timely release of generated gas (Figure 3(b, d)). It can be seen from the scanned image that the $Ni(OH)_2$ nanosheets are about 2.2 nm thick and about 10 atomic layers thick. The thickness of the nanosheets hardly changes after in-situ reduction (Figure 3(c, e)). It means that the 3D array electrode produced in situ has certain stability. When Ni array electrodes are used for hydrazine oxidation reaction (HzOR) and HER catalytic testing, the ultra-thin single-crystal layered Ni nanosheet array has better activity and stability than Pt/C. For polymetallic alloy array catalysts used for water electrolysis, CoNi alloy nanosheets array[69], NiMo alloy nanosheets array[70] are also used to study electrocatalytic activity. Brewer-Engel valence bond theory believes that alloying transition metals can make transition metals with free or half-empty d orbitals and transition metals with paired d electrons have a synergistic effect, which may improve the HER performance of the material[71].

5.2 Metal (hydro)oxide array catalyst

Transition metal materials have easy-to-adjust 3D electron orbits and are rich in earth content[72, 73]. The conductivity and stability of a single metal (hydro) oxide are insufficient, polymetallic (hydro) oxide are used to explore the corresponding electrochemical activity[74]. Layered double hydroxide (LDH) has become a representative of multi-metal compound catalyst materials[75]. In theory, as long as the radii of the divalent metal ion and the trivalent metal ion are similar, the corresponding LDH material can be formed. In experiments, LDH is generally controlled by adjusting the composition and content of the precursor solution[76]. There are many ways to synthesize LDH, the common ones are co-precipitation, electrodeposition, hydrothermal synthesis and so on. In recent research reports, combining LDH with a conductive substrate to form a catalytic electrode with a 3D array structure has become a new research topic[77].

Li et al. used a simple hydrothermal process to self-grown Co_3O_4 nanorod arrays on the surface of carbon cloth (CC), and constructed an amorphous Co-P layer on the surface of the array structure by cathodic polarization[78]. When performing the HER test in 1 $mol \cdot L^{-1}$ KOH, the Co_3O_4 nanorod array electrode coated with Co-P only needs 73 mV to reach a current density of 10 $mA \cdot cm^{-2}$, while the uncoated Co_3O_4 requires 260 mV(Figure 4(a)). The Tafel slope of Co-

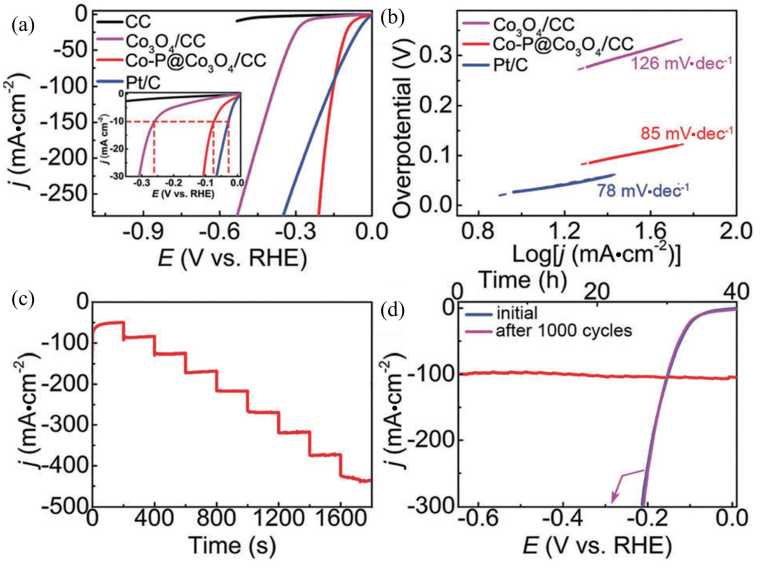

Figure 4. The electrochemical performance of Co-P@ Co_3O_4/CC. (a) The polarization curves and (b) the Tafel slopes of different materials. (c) The multi-step chronopotentiometric curve and (d) the contrast polarization curve before and after 1000 cycles of cyclic voltammetry and the stability test with a current density of 100 mA · cm^{-2} of Co-P@ Co_3O_4/CC. Reproduced with permission from Ref. [78]. Copyright 2018, The Royal Society of Chemistry.

P@ Co_3O_4/CC is much lower than that of Co_3O_4/CC, which means the rapid HER kinetics (Figure 4(b)). In the multi-step chrono-potentiometric test, the modified Co_3O_4 array maintains a stable current density at each potential (Figure 4(c)). Even the high current density of 100 mA · cm^{-2} is stable for more than 40 h (Figure 4(d)), which fully shows that this 3D array electrode has an excellent mass transfer, electrical conductivity and mechanical stability. In addition, CoOOH nanoarrays were also synthesized and used in OER reactions[79].

In recent years, multi-metal (hydro) oxide arrays for electrolysis of water have also been studied. Xue et al. used a simple electrochemical deposition process to grow MFe-LDH (M=Ni, Co and Li) nanosheet arrays with a thickness of about 10 nm on different conductive substrates[80]. This kind of catalytic electrode synthesized in a short time at a room temperature exhibits excellent OER activity. The current density of 10 mA · cm^{-2} only needs a potential of 224 mV, which is better than that of Ir/C catalytic materials. In the previous work, the NF was directly immersed in a mixed solution containing a certain concentration of iron nitrates and cobalt nitrates, where iron nitrates, cobalt nitrates and NF were the source of Fe, Co and Ni elements, respectively[81]. Take advantage of the etching effect of Fe^{3+} on NF, an amorphous Fe-Co-Ni hydroxide nanosheet array is directly grown on the surface of the NF. When the OER is carried out under alkaline conditions, the nanosheet array electrode obtained by the simple co-precipitation method needs only 212 mV and 319 mV overpotentials to achieve current densities of 10 and 100 mA · cm^{-2}, respectively. It is much smaller than the overpotential of 297 mV required for the commercial RuO_2 to reach 10 mA · cm^{-2}. In addition to the hydroxide nanoarray materials mentioned above, oxide array materials such as Co_3O_4 nanotube arrays with hollow structures[82], NiO nanorod arrays containing oxygen vacancies[17], and NiO nanosheet arrays treated with N_2-plasma[83] have also been used to explore their corresponding electrocatalytic activity.

5.3 Metal sulfide array catalyst

Metal sulfides are generally produced by the reaction of sulfur and metals, and can also be produced by the reaction of hydrogen sulfide gas with metal (hydro) oxides[63]. They are generally insoluble in water and are relatively stable compared with metal (hydro) oxides. Metal sulfides have more chemical composition, crystal structure and valence state, showing more structural shapes, higher electrical conductivity and mechanical strength. Thanks to the unique sheet morphology and stable physic-chemical properties, the layered metal sulfide has the advantages of large specific surface area to be exposed to active sites, which has great application potential in the field of electrochemistry[84]. Liu et al. combined MoS_2 nanosheet arrays with CC through a one-step hydrothermal method[85]. The vertically arranged MoS_2 nanosheet arrays will not aggregate like the powder materials, effectively exposed to more active sites and exhibiting a better catalytic activity.

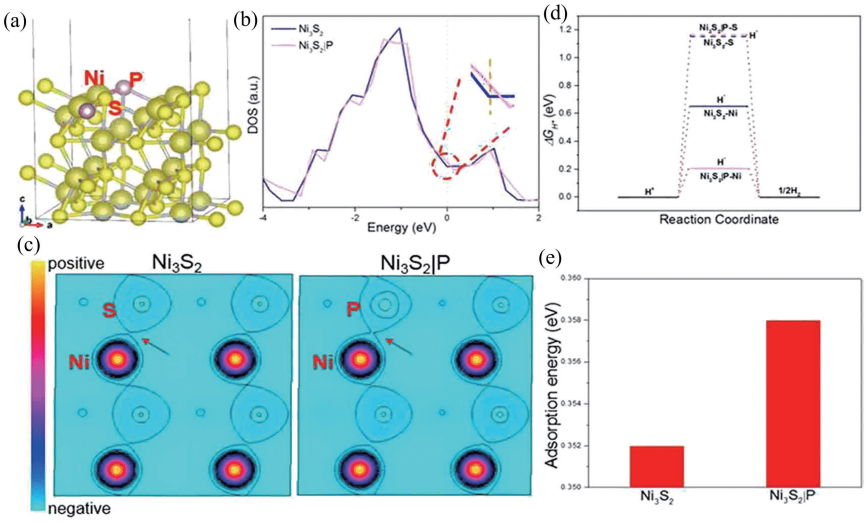

Figure 5. DFT calculation of $Ni_3S_2|P$. (a) Optimized crystal structure of $Ni_3S_2|P$. (b) The calculated density of states, the Fermi level is set to 0 eV. (c) The distribution of charge density, which black line represents the contour line of the charge density. (d) The HER free energy diagram calculated under equilibrium potential. (e) The adsorption energy required for H_2O molecules adsorbed on Ni sites. Reproduced with permission from Ref. [43]. Copyright 2018, American Chemical Society.

Ni_3S_2 has low inherent resistivity, which gives it the advantage of rapid electron transfer in electrocatalytic testing. The P element was doped into the Ni_3S_2 matrix to adjust its original electronic state[43]. According to the density functional theory results, it can be seen from the optimized crystal structure of $P|Ni_3S_2$ (Figure 5(a)) and the calculated density of states (Figure 5(b)) that the P incorporated Ni_3S_2 array still maintains the metallic properties, which is conducive to the rapid transmission of electrons. In detail, the incorporation of P element induces more electronic states resulting in a higher charge density (Figure 5(c)). Taking Ni as the active site and calculating the corresponding hydrogen adsorption Gibbs free energy, $P|Ni_3S_2$ only requires 0.197 eV, which is much smaller than the 0.6 eV required by Ni_3S_2 (Figure 5(d)). At the same time, P modification can also provide a higher level of water binding energy (Figure 5(e)). Therefore, the $P|Ni_3S_2$ array electrode grown on the NF is suitable for the catalyst of the hydrolysis reaction. Al-doped nickel sulfide nanosheet arrays[86], $FeCo_2S_4$ nanosheet arrays[87], and Co_3S_4 nanorod arrays combined with MoS_2 nanosheets[88] have all been proven to be effective catalyst materials for overall water decomposition.

5.4 Metal selenide array catalyst

In the periodic table of chemical elements, both selenium and sulfur belong to VI A group. Since the outer electrons of the element determine the strength of its bond with hydrogen, metal selenides and sulfides have similar chemical properties. Mai et al. synthesized NiFe selenide nanosheet arrays with porous structure by the selenization treatment of NiFe-LDH[89]. When performing OER testing under alkaline conditions, this 3D porous array electrode only needs an overpotential of 255 mV to reach a current density of 35 mA · cm^{-2}. The incorporation of Fe and the selenization process ensure the rapid transport of electrons, while the porous structure exposes a greater number of active sites. Gao's research group also partially selenized the CoNi-LDH array to synthesize a CoNiSe-CoNi LDH array with a heterogeneous structure[90], which has the excellent stability for more than 48 h during the hydrolysis experiment. $MoSe_2/CoSe_2$ hybrid nanoarrays also showed a high HER activity and stability[91].

5.5 Metal phosphide array catalyst

Metal phosphides have high mechanical strength, good electrical conductivity and relatively stable chemical properties, and their catalytic activity is better than other metal compounds. Related studies have shown that phosphorus atoms in phosphides are negatively charged and can capture positively charged protons during the electrocatalytic hydrogen evolution process[84, 92]. Therefore, phosphorus atoms play a very important role in the process of electrolysis of water[93]. The commonly used methods for the synthesis of phosphides include hydrothermal synthesis and high temperature synthesis. Phytic acid, triphenylphosphine, sodium hypophosphite, phosphoric acid and red phosphorus are all commonly used phosphorus sources. Among them, the organic phosphorus source is generally coated on the surface of the material, and a higher temperature is required to form phosphide. The inorganic phosphorus source generally generates phosphine gas before phosphating the material. But phosphine gas is very

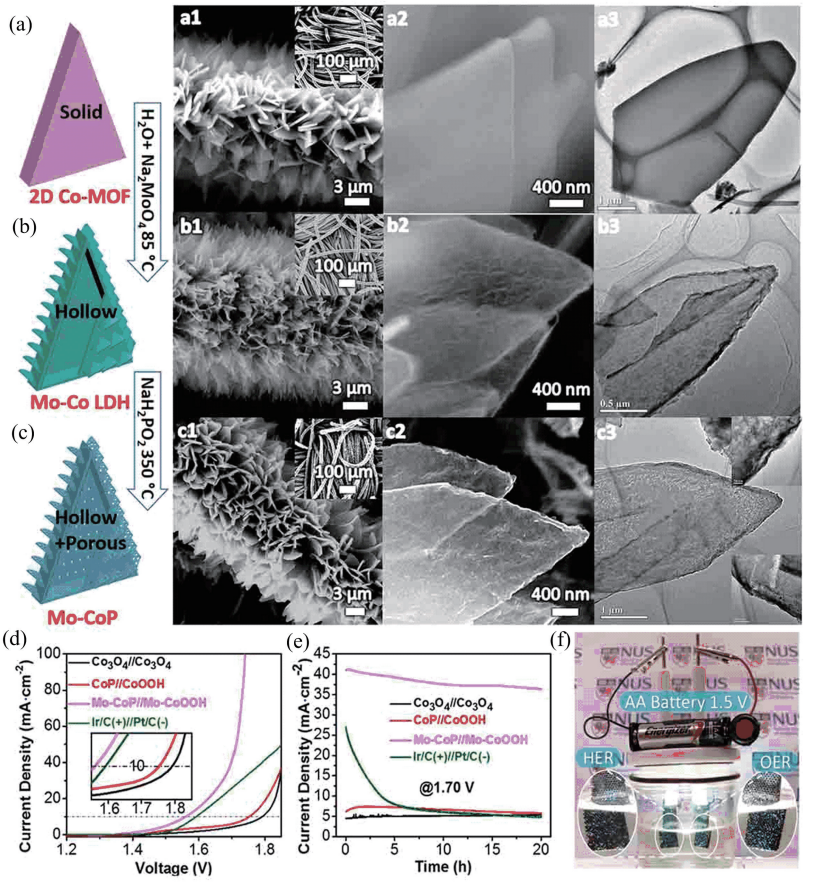

Figure 6. Synthetic schematic and characterization of Mo-doped CoP array. Pictures of structural model and corresponding micmorphology images of (a) Co-MOF nanoarray; (b) Mo-Co LDH array; (c) Mo-CoP nanoarray. The electrochemical test of overall water decomposition under alkaline conditions. (d) Polarization curve. (e) Stability test curve. (f) Photograph of the electrolysis water test driven by a 1.5 V DC battery. Reproduced with permission from Ref. [96]. Copyright 2017, John Wiley and Sons.

dangerous, and it is necessary to keep the gas circulating during the phosphating process[94].

Lu et al. successively grew cobalt phosphide nanosheet arrays on N-doped graphene through a hydrothermal process and a high-temperature phosphating process[95]. Guan et al. first grew Co-MOF as a precursor on CC (Figure 6(a)), then converted it into a CoMo-LDH array in situ (Figure 6(b)), and finally formed the Mo-CoP nano-array catalytic electrode through phosphating treatment (Figure 6(c))[96]. When the electrocatalytic test is performed in an alkaline environment (pH = 14), the current density of 10 mA · cm^{-2} for HER and OER requires overpotentials of 40 and 305 mV, respectively. Studies have found that Mo-doped CoP will be converted to Mo-CoOOH during the OER reaction, and the doped Mo atoms accelerate the electron transfer rate and improve the catalytic efficiency. When Mo-CoP and Mo-CoOOH electrode are respectively used as the cathode and anode to assemble the water electrolysis device for testing, Mo-CoP//Mo-CoOOH only needs 1.56 V to drive the current density of 10 mA · cm^{-2}, which is 15 mV lower than the performance of the catalyst composed of noble materials (Figure 6(d)). The stability is also better than other contrast samples (Figure 6(e)). When a 1.5 V DC battery is used to drive the complete hydrolysis reaction, the precipitation of hydrogen and oxygen can be clearly seen. The electrocatalytic properties of copper phosphide nanoarrays[97], tungsten phosphide nanorod arrays[98], iron phosphide nanorod arrays[99] and molybdenum phosphide nanosheet arrays[100] electrodes have also been reported. Metal phosphides are proven to be excellent catalyst materials.

5.6 Metal nitride array catalyst

Nitrogen is located in the second period of the periodic table. The radius of nitrogen atom is too small to be embedded in the metal lattice gap, therefore the metal nitride maintains the characteristics of metal with great conductivity. Similar to the preparation of metal phosphides, Li et al. first grew CoFe-LDH nanosheet arrays in situ on the surface of NF, and then nitriding treatment is carried out in ammonia atmosphere to prepare CoFe nitride nanosheet arrays with porous

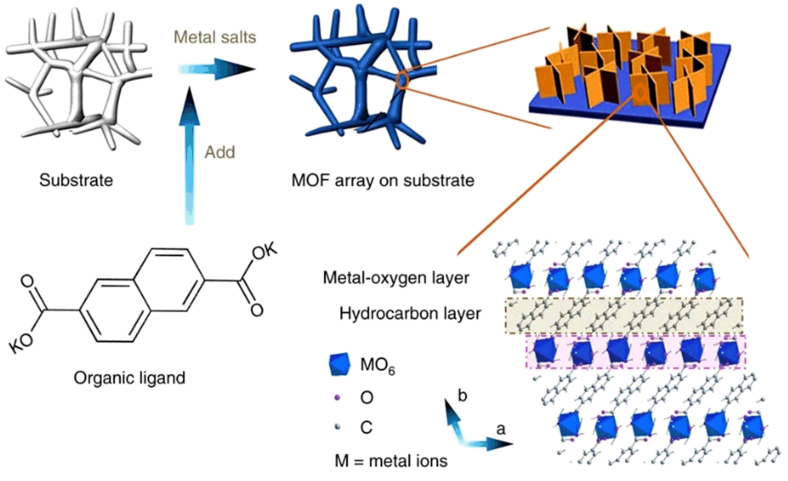

Figure 7. Synthesis method of MOF array composite material. Reproduced with permission from Ref. [107]. Copyright 2017, Springer Nature.

structures[101]. The porous structure exposes a larger number of active sites to participate in the electrocatalytic reaction, which cooperates with the conductive substrate to effectively enhance the activity of the electrolyzed water. Lei et al. grew CoN/Cu_3N nanotube arrays in situ on the surface of the foamed copper[102]. Nitriding treatment effectively improved the conductive properties of the precursor, exposing more active sites, and greatly improving the dynamic characteristics of OER and HER. In the bimetallic CoMo nitride nanosheet arrays, Mo_2N and Co_2N synergistically promote the water splitting reaction, only a voltage of 1.55 V can drive a current density of 10 mA · cm^{-2}[103]. The research of these stable metal nitride arrays provides new ideas for the exploration of new electrocatalysts.

5.7 Metal carbide array catalyst

Metal carbides have been widely concerned by electrocatalytic research because of their similar electronic structure to Pt[104]. They are generally formed at higher temperatures, which inevitably lead to sintering and agglomeration of catalytic materials. Distributing the metal carbides vertically on the conductive substrate avoids the aggregation of active materials and exposes a large number of active sites. Therefore, designing a metal carbide array electrode with an array structure is beneficial to increase the contact area between the catalyst and the reaction medium. Metal carbide arrays for electrocatalytic reactions have also been reported. Wang et al. have synthesized W-based carbide nanosheet arrays on CC, which are used in both HER and OER catalysts[105]. The Co_6W_6C nanosheet array catalytic material constructed with MOF as the precursor has a stability of more than 50 h when undergoing a complete hydrolysis reaction. The carbon-coated V_8C_7 array grown in situ on the surface of NF proved to have excellent catalytic performance similar to Pt[106].

5.8 MOF array catalyst

MOF refers to a crystalline porous material with a periodic network structure, which is formed by the self-assembly of transition metal ions and organic ligands. It has the characteristics of high porosity, large specific surface area, regular channels with adjustable pore size and diversity of a topological structure, and it usually exists in a powder form. However, MOF materials are considered unsuitable for electrochemistry due to poor conductivity. Combining MOF and conductive substrates to construct a 3D array composite material can effectively reduce the impact of low conductivity. Different MOF materials usually have different synthesis methods. Zhao et al. once introduced a general method for synthesizing MOF arrays with ultra-thin nanosheet structures on different substrates[107]. First, the metal salt ions and the substrate are mixed in the aqueous solution, and then the organic ligand is introduced, the MOF nanosheet array is grown on the surface of the substrate according to the dissolution crystallization mechanism (Figure 7). The 2D NiFe-MOF nanosheet on the NF fabricated by this method only needs an overpotential of 240 mV to drive a current density of 10 mA · cm^{-2}. During the stability test, the current hardly changed within 20000 s. Sun et al. used Fe^{3+} and terephthalic acid as raw materials to prepare a two-dimensional Fe-MOF nanosheet array by a one-step hydrothermal method[108]. When performing OER testing in 1 mol · L^{-1} KOH electrolyte, an overpotential of 240 and 270 mV is required to achieve current densities of 50 and 100 mA · cm^{-2}, respectively. The current density rises sharply at higher voltages.

6 Summary and outlook

With the deepening of research, more and more array

electrode materials for water electrolysis have been designed and prepared. Recent researches are shown in Table 1. The 3D array electrode composed of active material and conductive substrates is used as a catalyst for water electrolysis. Whether it is used for HER or OER testing, the overpotential required to achieve a current density of 10 mA · cm^{-2} is relatively small. It is at an excellent level in reports on electrolyzed water.

Table 1. Summary of electrocatalytic applications and performance of 3D array materials.

No.	Materials	Applications	Performance	Ref.
1	Pt−Co_2S/CC	HER (1mol · L^{-1} KOH)	24 mV @ 10 mA · cm^{-2}	[109]
		OER(1mol · L^{-1}KOH)	300 mV@ 10 mA · cm^{-2}	
2	Ru-Ni_2P/NF	HER (1 mol · L^{-1} KOH)	45 mV @ 10 mA · cm^{-2}	[110]
3	Ru-NiFe LDH-F/NF	HER (1mol · L^{-1} KOH)	115.6 mV @ 10 mA · cm^{-2}	[111]
		OER(1mol · L^{-1}KOH)	230 mV @ 10 mA · cm^{-2}	
4	0.1Pt-VS_2/CP	HER (0.5 mol · L^{-1} H_2SO_4)	77 mV @ 10 mA · cm^{-2}	[112]
5	$CaMoO_4$/NF	OER (1 mol · L^{-1} KOH)	345 mV @ 50 mA · cm^{-2}	[113]
6	Fe-Co-Ni hydroxide/NF	OER (1mol · L^{-1} KOH)	212 mV @ 10 mA · cm^{-2}	[81]
7	NiCoON/NF	OER (1 mol · L^{-1} KOH)	247 mV @ 10 mA · cm^{-2}	[114]
8	NiFe LDH NS/NF	OER (1 mol · L^{-1} KOH)	233 mV @ 30 mA · cm^{-2}	[115]
9	P-$Ni(OH)_2$/$NiMoO_4$/NF	HER (1 mol · L^{-1} KOH)	60 mV @ 10 mA · cm^{-2}	[116]
		OER (1 mol · L^{-1} KOH)	270 mV @ 10 mA · cm^{-2}	
10	NiCo-LDH@ HOS/NF	OER (0.1mol · L^{-1} KOH)	293 mV @ 10 mA · cm^{-2}	[117]
11	Ni-$NiFe_2O_4$/CC	OER (1 mol · L^{-1} KOH)	212 mV @ 10 mA · cm^{-2}	[118]
12	FeOOH NSAs/NF	OER (1 mol · L^{-1} KOH)	235 mV @ 10 mA · cm^{-2}	[119]
13	Ni-NSAs/NF	HER (0.1 mol · L^{-1} KOH)	35 mV @ onset potential	[68]
14	NC@ $CuCo_2N_x$/CF	HER (1 mol · L^{-1} KOH)	105 mV @ 10 mA · cm^{-2}	[120]
		OER (1 mol · L^{-1} KOH)	230 mV @ 10 mA · cm^{-2}	
15	NSP-Ni_3FeN/NF	HER (1 mol · L^{-1} KOH)	45 mV @ 10 mA · cm^{-2}	[121]
		OER (1 mol · L^{-1} KOH)	223 mV @ 10 mA · cm^{-2}	
16	CoNiB/CoNi Foam	OER (1 mol · L^{-1}KOH)	262 mV @ 10 mA · cm^{-2}	[122]
17	MoS_2 NA/CC	HER (0.5 mol · L^{-1} H_2SO_4)	140 mV @ onset potential	[85]
18	FeCoP NSA/NF	HER (1 mol · L^{-1} KOH)	160 mV @ 100 mA · cm^{-2}	[123]
		OER (1 mol · L^{-1} KOH)	330 mV @ 100 mA · cm^{-2}	
19	Fe-MOF/NF	OER (1 mol · L^{-1} KOH)	240 mV @ 50 mA · cm^{-2}	[108]
20	NiFe-MOF/NF	HER (0.1 mol · L^{-1} KOH)	134 mV @ 10 mA · cm^{-2}	[107]
		OER (0.1 mol · L^{-1} KOH)	240 mV @ 10 mA · cm^{-2}	

In this review, the reaction mechanism of HER and OER in the water electrolysis process is briefly described. Then several strategies commonly used to improve the catalytic performance of materials are summarized. Among them, the combination of active material and conductive substrates to form a composite working electrode has become a hot spot in the field of water electrolysis. Structurally speaking, the 3D array electrode has the advantages of preventing the accumulation of active materials, exposing more active sites, promoting the rapid transfer of electrons, accelerating the diffusion of reactive species, and releasing reaction gas in time. Most of the 3D array electrodes used for electrocatalysis are composed of

transition metal compounds. In the article, different kinds of array catalysts are listed, and some research progress of corresponding kinds of materials is discussed. A lot of 3D array electrodes for catalytic reactions have been studied, but their high manufacturing cost and complex synthesis process have become the main problems that limit their further development. Therefore, it is an important research direction to develop layered two-dimensional composite materials with a stable structure and excellent performance, suitable for large-scale preparation.

Acknowledgments

This work was supported by National Key R&D Program of China (2017YFA0207301), Youth Innovation Promotion Association CAS (Y202092), Fundamental Research Funds for the Central Universities (WK2340000094).

Conflict of interest

The authors declare no conflict of interest.

Author information

LIU Qilong is currently a research assistant at the Renewable Energy Research Center of the Institute of Energy, Hefei Comprehensive National Science Center. His research interests focus on the research of catalysts for the conversion of small energy molecules.

XIAO Chong obtained his PhD degree from the University of Science and Technology of China (USTC) in 2013. He is now a professor of Hefei National Laboratory for Physical Sciences at the Microscale, USTC. He has been working on advanced thermoelectric semiconductors for more than 8 years, regarding materials synthesis and characterization for understanding the underlying physics and chemistry mechanism. His recent research interests focus on the design and synthesis of low-dimensional inorganic solids with efforts to modulate their electron and phonon structures for energy storage and conversion applications.

References

[1] Suen N T, Hung S F, Quan Q, et al. Electrocatalysis for the oxygen evolution reaction: Recent development and future perspectives. Chemical Society Reviews, 2017, 46(2): 337-365.

[2] Seh Z W, Kibsgaard J, Dickens C F, et al. Combining theory and experiment in electrocatalysis: Insights into materials design. Science, 2017, 355:4998.

[3] Luo M, Guo S. Strain-controlled electrocatalysis on multimetallic nanomaterials. Nature Reviews Materials, 2017, 2(11): 17059.

[4] Chu S, Majumdar A. Opportunities and challenges for a sustainable energy future. Nature, 2012, 488(7411): 294-303.

[5] Trasatti S. Water electrolysis: Who first? Journal of Electroanalytical Chemistry, 1999, 476(1): 90-91.

[6] Levie R D. The electrolysis of water. Journal of Electroanalytical Chemistry, 1999, 476(1): 92-93.

[7] Benck J D, Hellstern T R, Kibsgaard J, et al. Catalyzing the hydrogen evolution reaction (HER) with molybdenum sulfide nanomaterials. ACS Catalysis, 2014, 4(11): 3957-3971.

[8] Zou X, Zhang Y. Noble metal-free hydrogen evolution catalysts for water splitting. Chemical Society Reviews, 2015, 44(15): 5148-5180.

[9] Huang Z F, Song J, Pan L, et al. Tungsten oxides for photocatalysis, electrochemistry, and phototherapy. Advanced Materials, 2015, 27(36): 5309-5327.

[10] Zhang X, Klaver P, Van Santen R, et al. Oxygen evolution at hematite surfaces: The impact of structure and oxygen vacancies on lowering the overpotential. The Journal of Physical Chemistry C, 2016, 120(32): 18201-18208.

[11] TONG S S, WANG X J, LI Q C, et al. Progress onelectrocatalysts of hydrogen evolution reaction based on carbon fiber materials. Chinese Journal of Analytical Chemistry, 2016, 44(9): 1447-1457.

[12] Cook T R, Dogutan D K, Reece S Y, et al. Solar energy supply and storage for the legacy and nonlegacy worlds . Chemical Reviews, 2010, 110(11): 6474-6502.

[13] Jin H, Guo C, Liu X, et al. Emerging two-dimensional nanomaterials for electrocatalysis. Chemical Reviews, 2018, 118(13): 6337-6408.

[14] Chen D, Zou Y, Wang S. Surface chemical-functionalization of ultrathin two-dimensional nanomaterials for electrocatalysis. Materials Today Energy, 2019, 12:250-268.

[15] Kong X, Liu Q, Zhang C, et al. Elemental two-dimensional nanosheets beyond graphene. Chemical Society Reviews, 2017, 46(8): 2127-2157.

[16] Guo X L, Zhang J M, Xu W N, et al. Growth of NiMn LDH nanosheet arrays on KCu_7S_4 microwires for hybrid supercapacitors with enhanced electrochemical performance. Journal of Materials Chemistry A, 2017, 5(39): 20579-20587.

[17] Zhang T, Wu M Y, Yan D Y, et al. Engineering oxygen vacancy on NiO nanorod arrays for alkaline hydrogen evolution. Nano Energy, 2018, 43:103-109.

[18] Wang X, Yu L, Guan B Y, et al. Metal-organic framework hybrid-assisted formation of Co_3O_4/Co-Fe oxide double-shelled nanoboxes for enhanced oxygen evolution. Advanced Materials, 2018, 30(29):1801211.

[19] Wu Y, Meng Y, Hou J, et al. Orienting active crystal planes of new class lacunaris Fe_2PO_5 polyhedrons for robust water oxidation in alkaline and neutral media. Advanced Functional Materials, 2018, 28(35): 1801397.

[20] Chaudhari N K, Jin H, Kim B, et al. Nanostructured materials on 3D nickel foam as electrocatalysts for water splitting. Nanoscale, 2017, 9(34): 12231-12247.

[21] Liu J, Zhu D, Zheng Y, et al. Self-supported earth-abundant nanoarrays as efficient and robust electrocatalysts

for energy-related reactions. ACS Catalysis, 2018, 8(7): 6707-6732.
[22] Sun X, Huo J, Yang Y, et al. The Co_3O_4 nanosheet array as support for MoS_2 as highly efficient electrocatalysts for hydrogen evolution reaction. Journal of Energy Chemistry, 2017, 26(6): 1136-1139.
[23] Faber M S, Jin S. Earth-abundant inorganic electrocatalysts and their nanostructures for energy conversion applications. Energy & Environmental Science, 2014, 7(11): 3519-3542.
[24] Fang M, Dong G, Wei R, et al. Hierarchical nanostructures: Design for sustainable water splitting. Advanced Energy Materials, 2017, 7(23): 1700559.
[25] Jiao Y, Zheng Y, Jaroniec M, et al. Design of electrocatalysts for oxygen- and hydrogen-involving energy conversion reactions. Chemical Society Reviews, 2015, 44(8): 2060-2086.
[26] Kibler L A. Hydrogen electrocatalysis. ChemPhysChem, 2006, 7(5): 985-991.
[27] Li Y, Wang H, Xie L, et al. MoS_2 nanoparticles grown on graphene: An advanced catalyst for the hydrogen evolution reaction. Journal of the American Chemistry Society, 2011, 133(19): 7296-7299.
[28] Zhao G, Sun Y, Zhou W, et al. Superior photocatalytic H_2 production with cocatalytic Co/Ni species anchored on sulfide semiconductor. Advanced Materials, 2017, 29(40): 1703258.
[29] Staszak-Jirkovsky J, Malliakas C D, Lopes P P, et al. Design of active and stable Co-Mo-Sx chalcogels as pH-universal catalysts for the hydrogen evolution reaction. Nature Materials, 2016, 15(2): 197-203.
[30] Kim J S, Kim B, Kim H, et al. Recent progress on multimetal oxide catalysts for the oxygen evolution reaction. Advanced Energy Materials, 2018, 8(11):1702774.
[31] Rossmeisl J, Logadottir A, Nørskov J K. Electrolysis of water on (oxidized) metal surfaces. Chemical Physics, 2005, 319: 178-184.
[32] Man I C, Su H Y, Calle-Vallejo F, et al. Universality in oxygen evolution electrocatalysis on oxide surfaces. ChemCatChem, 2011, 3(7): 1159-1165.
[33] Xu Z, Rossmeisl J, Kitchin J R. A Linear response DFT+U study of trends in the oxygen evolution activity of transition metal rutile dioxides. The Journal of Physical Chemistry C, 2015, 119(9): 4827-4833.
[34] Cheng F, Su Y, Liang J, et al. MnO_2-based nanostructures as catalysts for electrochemical oxygen reduction in alkaline media. Chemistry of Materials, 2010, 22(3): 898-905.
[35] Ma T Y, Dai S, Jaroniec M, et al. Metal-organic framework derived hybrid Co_3O_4-carbon porous nanowire arrays as reversible oxygen evolution electrodes. Journal of the American Chemistry Society, 2014, 136(39): 13925-13931.
[36] Li J, Yang Z, Lin Y, et al. Self-supported molybdenum doping Ni_3S_2 nanoneedles as efficient bifunctional catalysts for overall water splitting. New Journal of Chemistry, 2020, 44(20): 8578-8586.
[37] Zhang J, Song M, Wang J, et al. In-situ transformation to accordion-like core-shell structured metal @ metallic hydroxide nanosheet from nanorod morphology for overall water-splitting in alkaline media. Journal of Colloid and Interface Science, 2020, 559:105-114.
[38] Aqueel Ahmed A T, Pawar S M, InamdarA I, et al. A morphologically engineered robust bifunctional $CuCo_2O_4$ nanosheet catalyst for highly efficient overall water splitting. Advanced Materials Interfaces, 2019, 7(2): 1901515.
[39] Guo C, Liu X, Gao L, et al. Fe-doped Ni_2P nanosheets with porous structure for electroreduction of nitrogen to ammonia under ambient conditions. Applied Catalysis B: Environmental, 2020, 263:118296.
[40] Niu H J, Zhang L, Feng J J, et al. Graphene-encapsulated cobalt nanoparticles embedded in porous nitrogen-doped graphitic carbon nanosheets as efficient electrocatalysts for oxygen reduction reaction. Journal of Colloid and Interface Science, 2019, 552:744-751.
[41] Zhang J, Zhang M, Zeng Y, et al. Single Fe atom on hierarchically porous S, N-codoped nanocarbon derived from porphyra enable boosted oxygen catalysis for rechargeable Zn-air batteries. Small, 2019, 15(24): 1900307.
[42] Zhang H, Liu Q, Xu J, et al. Holey ruthenium nanosheets with moderate aluminum modulation toward hydrogen evolution. Inorg Chem, 2019, 58(13): 8267-8270.
[43] Liu Q, Wei L, Liu Q, et al. Anion engineering on 3D Ni_3S_2 nanosheets array toward water splitting. ACS Applied Energy Materials, 2018, 1(7): 3488-3496.
[44] Wu Z, Nie D, Song M, et al. Facile synthesis of Co-Fe-B-P nanochains as an efficient bifunctional electrocatalyst for overall water-splitting. Nanoscale, 2019, 11(15): 7506-7512.
[45] Chen C, Yan D, Wang Y, et al. BN pairs enriched defective carbon nanosheets for ammonia synthesis with high efficiency. Small, 2019, 15(7): 1805029.
[46] Liu Q, Liu Q, Kong X. Anion engineering on free-standing two-dimensional MoS_2 nanosheets toward hydrogen evolution. Inorganic Chemistry, 2017, 56(19): 11462-11465.
[47] Duan J J, Han Z, Zhang R L, et al. Iron, manganese co-doped Ni_3S_2 nanoflowers in situ assembled by ultrathin nanosheets as a robust electrocatalyst for oxygen evolution reaction. Journal of Colloid and Interface Science, 2021, 588:248-256.
[48] Nadeem M, Yasin G, Arif M, et al. Highly active sites of Pt/Er dispersed N-doped hierarchical porous carbon for trifunctional electrocatalyst. Chemical Engineering Journal, 2021, 409:128205.
[49] Jin Q, Ren B, Cui H, et al. Nitrogen and cobalt co-doped carbon nanotube films as binder-free trifunctional electrode for flexible zinc-air battery and self-powered overall water splitting. Applied Catalysis B: Environmental, 2021, 283: 119643.
[50] Mohammed-Ibrahim J, Sun X. Recent progress on earth abundant electrocatalysts for hydrogen evolution reaction (HER) in alkaline medium to achieve efficient water splitting: A review. Journal of Energy Chemistry, 2019, 34:111-160.
[51] Wang G, Ling Y, Wang H, et al. Hydrogen-treated WO_3 nanoflakes show enhanced photostability. Energy & Environmental Science, 2012, 5(3): 6180-6187.
[52] Bai S, Zhang N, Gao C, et al. Defect engineering in

photocatalytic materials. Nano Energy, 2018, 53:296-336.
[53] Ou G, Xu Y, Wen B, et al. Tuning defects in oxides at room temperature by lithium reduction. Nature Communication, 2018, 9(1): 1302.
[54] Xu L, Jiang Q, Xiao Z, et al. Plasma-engraved Co_3O_4 nanosheets with oxygen vacancies and high surface area for the oxygen evolution reaction. Angewandte Chemie International Edition in English, 2016, 55(17): 5277-5281.
[55] Tao L, Duan X, Wang C, et al. Plasma-engineered MoS_2 thin-film as an efficient electrocatalyst for hydrogen evolution reaction. Chemical Communication (Camb), 2015, 51(35): 7470-7473.
[56] Li C, Ma D, Mou S, et al. Porous $LaFeO_3$ nanofiber with oxygen vacancies as an efficient electrocatalyst for N_2 conversion to NH_3 under ambient conditions. Journal of Energy Chemistry, 2020, 50:402-408.
[57] Tong Y, Guo H, Liu D, et al. Vacancy engineering of iron-doped $W_{18}O_{49}$ nanoreactors for low-barrier electrochemical nitrogen reduction. Angewandte Chemie International Edition in English, 2020, 59(19): 7356-7361.
[58] Li Y B, Liu Y P, Wang J, et al. Plasma-engineered NiO nanosheets with enriched oxygen vacancies for enhanced electrocatalytic nitrogen fixation. Inorganic Chemistry Frontiers, 2020, 7(2): 455-463.
[59] Bolar S, Shit S, Murmu N C, et al. Doping-assisted phase changing effect on MoS_2 towards hydrogen evolution reaction in acidic and alkaline pH. ChemElectroChem, 2020, 7(1): 336-346.
[60] Voiry D, Salehi M, Silva R, et al. Conducting MoS_2 nanosheets as catalysts for hydrogen evolution reaction. Nano Letters, 2013, 13(12): 6222-6227.
[61] Qu M, Jiang Y, Yang M, et al. Regulating electron density of NiFe-P nanosheets electrocatalysts by a trifle of Ru for high-efficient overall water splitting. Applied Catalysis B: Environmental, 2020, 263:118324.
[62] Liang C, Zou P, Nairan A, et al. Exceptional performance of hierarchical Ni-Fe oxyhydroxide@NiFe alloy nanowire array electrocatalysts for large current density water splitting. Energy & Environmental Science, 2020, 13(1): 86-95.
[63] Lin J, Wang P, Wang H, et al. Defect-rich heterogeneous MoS_2/NiS_2 nanosheets electrocatalysts for efficient overall water splitting. Advanced Science, 2019, 6(14): 1900246.
[64] Mccrory C C, Jung S, Ferrer I M, et al. Benchmarking hydrogen evolving reaction and oxygen evolving reaction electrocatalysts for solar water splitting devices. Journal of the American Chemistry Society, 2015, 137(13): 4347-4357.
[65] Wang X, Zhang Y, Si H, et al. Single-atom vacancy defect to trigger high-efficiency hydrogen evolution of MoS_2. Journal of the American Chemistry Society, 2020, 142(9): 4298-4308.
[66] Huang Z, Chen Z, Chen Z, et al. Cobalt phosphide nanorods as an efficient electrocatalyst for the hydrogen evolution reaction. Nano Energy, 2014, 9:373-382.
[67] Shi Q, Zhu C, Du D, et al. Robust noble metal-based electrocatalysts for oxygen evolution reaction. Chemical Society Reviews, 2019, 48(12): 3181-3192.
[68] Kuang Y, Feng G, Li P, et al. Single-crystalline ultrathin nickel nanosheets array from in situ topotactic reduction for active and stable electrocatalysis. Angewandte Chemie International Edition in English, 2016, 55(2): 693-697.
[69] Cheng C, Zheng F, Zhang C, et al. High-efficiency bifunctional electrocatalyst based on 3D freestanding Cu foam in situ armored CoNi alloy nanosheet arrays for overall water splitting. Journal of Power Sources, 2019, 427:184-193.
[70] Zhang Q, Li P, Zhou D, et al. Superaerophobic ultrathin Ni-Mo alloy nanosheet array from in situ topotactic reduction for hydrogen evolution reaction. Small, 2017, 13(41): 1701648.
[71] Zhou D, Li P, Xu W, et al. Recent advances in non-precious metal-based electrodes for alkaline water electrolysis. ChemNanoMat, 2020, 6(3): 336-355.
[72] Hu F, Zhu S, Chen S, et al. Amorphous metallic NiFeP: A conductive bulk material achieving high activity for oxygen evolution reaction in both alkaline and acidic media. Advanced Materials, 2017, 29(32): 1606570.
[73] Trotochaud L, Young S L, Ranney J K, et al. Nickel-iron oxyhydroxide oxygen-evolution electrocatalysts: The role of intentional and incidental iron incorporation. Journal of the American Chemistry Society, 2014, 136(18): 6744-6753.
[74] Wang B, Tang C, Wang H F, et al. A nanosized CoNi hydroxide@hydroxysulfide core-shell heterostructure for enhanced oxygen evolution. Advanced Materials, 2019, 31(4): 1805658.
[75] Gong M, Li Y G, Wang H L, et al. An advanced Ni-Fe layered double hydroxide electrocatalyst for water oxidation. Journal of the American Chemical Society, 2013, 135(23): 8452-8455.
[76] Jia H, Wang Z, Zheng X, et al. Interlaced Ni-Co LDH nanosheets wrapped Co_9S_8 nanotube with hierarchical structure toward high performance supercapacitors. Chemical Engineering Journal, 2018, 351:348-355.
[77] Yang R, Zhou Y, Xing Y, et al. Synergistic coupling of CoFe-LDH arrays with NiFe-LDH nanosheet for highly efficient overall water splitting in alkaline media. Applied Catalysis B: Environmental, 2019, 253:131-139.
[78] Ang L, Zhou H, Qin X, et al. Cathodic electrochemical activation of Co_3O_4 nanoarrays: A smart strategy to significantly boost the hydrogen evolution activity. Chemical Communication, 2018, 54(17): 2150-2153.
[79] Chen Z, Kronawitter C X, Yeh Y W, et al. Activity of pure and transition metal-modified CoOOH for the oxygen evolution reaction in an alkaline medium. Journal of Materials Chemistry A, 2017, 5(2): 842-850.
[80] Li Z, Shao M, An H, et al. Fast electrosynthesis of Fe-containing layered double hydroxide arrays toward highly efficient electrocatalytic oxidation reactions. Chemical Science, 2015, 6(11): 6624-6631.
[81] Liu Q, Zhang H, Xu J, et al. Facile preparation of amorphous Fe-Co-Ni hydroxide arrays: A highly efficient integrated electrode for water oxidation. Inorganic Chemistry, 2018, 57(24): 15610-15617.
[82] Zhu Y P, Ma T Y, Jaroniec M, et al. Self-templating synthesis of hollow Co_3O_4 microtube arrays for highly efficient water electrolysis. Angewandte Chemie International Edition in English, 2017, 56(5): 1324-1328.

[83] Sai K N S, Tang Y, Dong L, et al. N_2 plasma-activated NiO nanosheet arrays with enhanced water splitting performance. Nanotechnology, 2020, 31(45): 455709
[84] Joo J, Kim T, Lee J, et al. Morphology-controlled metal sulfides and phosphides for electrochemical water splitting. Advanced Materials, 2019, 31(14): 1806682.
[85] Kong Q, Wang X, Tang A, et al. Three-dimensional hierarchical MoS_2 nanosheet arrays/carbon cloth as flexible electrodes for high-performance hydrogen evolution reaction. Materials Letters, 2016, 177: 139-142.
[86] He W, Wang F, Jia D, et al. Al-doped nickel sulfide nanosheet arrays as highly efficient bifunctional electrocatalysts for overall water splitting. Nanoscale, 2020, 12(47): 24244-24250.
[87] Gong Y, Pan H, Xu Z, et al. Crossed $FeCo_2S_4$ nanosheet arrays grown on 3D nickel foam as high-efficient electrocatalyst for overall water splitting. International Journal of Hydrogen Energy, 2018, 43(36): 17259-17264.
[88] Sivanantham A, Ganesan P, Shanmugam S. Hierarchical $NiCo_2S_4$ nanowire arrays supported on Ni foam: An efficient and durable bifunctional electrocatalyst for oxygen and hydrogen evolution reactions. Advanced Functional Materials, 2016, 26(26): 4661-4672.
[89] Wang Z, Li J, Tian X, et al. Porous nickel-iron selenide nanosheets as highly efficient electrocatalysts for oxygen evolution reaction. ACS Applied Materials & Interfaces, 2016, 8(30): 19386-19392.
[90] Yang Y, Zhang W, Xiao Y, et al. $CoNiSe_2$ heteronanorods decorated with layered-double-hydroxides for efficient hydrogen evolution. Applied Catalysis B: Environmental, 2019, 242:132-139.
[91] Wang Y, Jian C, He X, et al. Self-supported molybdenum selenide nanosheets grown on urchin-like cobalt selenide nanowires array for efficient hydrogen evolution. International Journal of Hydrogen Energy, 2020, 45(24): 13282-13289.
[92] Kibsgaard J, Tsai C, Chan K, et al. Designing an improved transition metal phosphide catalyst for hydrogen evolution using experimental and theoretical trends. Energy & Environmental Science, 2015, 8(10): 3022-3029.
[93] Kibsgaard J, Jaramillo T F. Molybdenum phosphosulfide: An active, acid-stable, earth-abundant catalyst for the hydrogen evolution reaction. Angewandte Chemie International Edition in English, 2014, 53(52): 14433-14437.
[94] Ji L, Wang J, Teng X, et al. CoP nanoframes as bifunctional electrocatalysts for efficient overall water splitting . ACS Catalysis, 2019, 10(1): 412-419.
[95] Lu Y, Hou W, Yang D, et al. CoP nanosheets in-situ grown on N-doped graphene as an efficient and stable bifunctional electrocatalyst for hydrogen and oxygen evolution reactions. Electrochimica Acta, 2019, 307:543-552.
[96] Guan C, Xiao W, Wu H, et al. Hollow Mo-doped CoP nanoarrays for efficient overall water splitting. Nano Energy, 2018, 48:73-80.
[97] Hou C C, Chen Q Q, Wang C J, et al. Self-supported cedarlike semimetallic Cu_3P nanoarrays as a 3D high-performance Janus electrode for both oxygen and hydrogen evolution under basic conditions. ACS Applied Materials & Interfaces, 2016, 8(35): 23037-23048.
[98] Pu Z, Liu Q, Asiri A M, et al. Tungsten phosphide nanorod arrays directly grown on carbon cloth: A highly efficient and stable hydrogen evolution cathode at all pH values. ACS Applied Materials & Interfaces, 2014, 6(24): 21874-21879.
[99] Liang Y, Liu Q, Asiri A M, et al. Self-supported FeP nanorod arrays: A cost-effective 3D hydrogen evolution cathode with high catalytic activity. ACS Catalysis, 2014, 4(11): 4065-4069.
[100] Zhu W, Tang C, Liu D, et al. A self-standing nanoporous MoP_2 nanosheet array: An advanced pH-universal catalytic electrode for the hydrogen evolution reaction. Journal of Materials Chemistry A, 2016, 4(19): 7169-7173.
[101] Li D, Xing Y, Yang R, et al. Holey cobalt-iron nitride nanosheet arrays as high-performance bifunctional electrocatalysts for overall water splitting. ACS Applied Materials & Interfaces, 2020, 12(26): 29253-29263.
[102] Li J, Kong X, Jiang M, et al. Hierarchically structured CoN/Cu_3N nanotube array supported on copper foam as an efficient bifunctional electrocatalyst for overall water splitting. Inorganic Chemistry Frontiers, 2018, 5(11): 2906-2913.
[103] Lu Y, Li Z, Xu Y, et al. Bimetallic Co-Mo nitride nanosheet arrays as high-performance bifunctional electrocatalysts for overall water splitting. Chemical Engineering Journal, 2021, 411:128433.
[104] Ma Y Y, Lang Z L, Yan L K, et al. Highly efficient hydrogen evolution triggered by a multi-interfacial Ni/WC hybrid electrocatalyst. Energy & Environmental Science, 2018, 11(8): 2114-2123.
[105] Chen J, Ren B, Cui H, et al. Constructing pure phase tungsten-based bimetallic carbide nanosheet as an efficient bifunctional electrocatalyst for overall water splitting. Small, 2020, 16(23): 1907556.
[106] Xu H, Wan J, ZhangH, et al. A new platinum-like efficient electrocatalyst for hydrogen evolution reaction at all pH: Single-crystal metallic interweaved V_8C_7 networks. Advanced Energy Materials, 2018, 8(23): 1800575.
[107] Duan J, Chen S, Zhao C. Ultrathin metal-organic framework array for efficient electrocatalytic water splitting . Nature Communication, 2017, 8:15341.
[108] Zhang X X, Liu Q,Shi X F, et al. An Fe-MOF nanosheet array with superior activity towards the alkaline oxygen evolution reaction. Inorganic Chemistry Frontiers, 2018, 5(6): 1405-1408.
[109] Han X, Wu X, Deng Y, et al. Ultrafine Pt nanoparticle-decorated pyrite-type CoS_2 nanosheet arrays coated on carbon cloth as a bifunctional electrode for overall water splitting. Advanced Energy Materials, 2018, 8(24): 1800935.
[110] Wei C, Fan X, Deng X, et al. Ruthenium doped Ni_2P nanosheet arrays for active hydrogen evolution in neutral and alkaline water. Sustainable Energy & Fuels, 2020, 4(4): 1883-1890.
[111] Wang Y, Zheng P, Li M, et al. Interfacial synergy between dispersed Ru sub-nanoclusters and porous NiFe layered double hydroxide on accelerated overall water

splitting by intermediate modulation. Nanoscale, 2020, 12: 9669-9679.
[112] Zhu J, Cai L, Yin X, et al. Enhanced electrocatalytic hydrogen evolution activity in single-atom Pt-decorated VS_2 nanosheets. ACS Nano, 2020, 14(5):5600-5608.
[113] Gou Y, Liu Q, Shi X, et al. $CaMoO_4$ nanosheet arrays for efficient and durable water oxidation electrocatalysis under alkaline conditions. Chemical Communication, 2018, 54(40): 5066-5069.
[114] Li Y, Hu L, Zheng W, et al. Ni/Co-based nanosheet arrays for efficient oxygen evolution reaction. Nano Energy, 2018, 52:360-368.
[115] Xie J, Qu H, Lei F, et al. Partially amorphous nickel-iron layered double hydroxide nanosheet arrays for robust bifunctional electrocatalysis. Journal of Materials Chemistry A, 2018, 6(33): 16121-16129.
[116] Xi W, Yan G, Tan H, et al. Superaerophobic P-doped $Ni(OH)_2/NiMoO_4$ hierarchical nanosheet arrays grown on Ni foam for electrocatalytic overall water splitting. Dalton Transactions, 2018, 47(26): 8787-8793.
[117] Xiang K, Guo J, Xu J, et al. Surface sulfurization of NiCo-layered double hydroxide nanosheets enable superior and durable oxygen evolution electrocatalysis. ACS Applied Energy Materials, 2018, 1(8): 4040-4049.
[118] Zhang J, Jiang Y, Wang Y, et al. Ultrathin carbon coated mesoporous $Ni\text{-}NiFe_2O_4$ nanosheet arrays for efficient overall water splitting. Electrochimica Acta, 2019, 321: 134652.
[119] Ma P, Luo S, Luo Y, et al. Vertically aligned FeOOH nanosheet arrays on alkali-treated nickel foam as highly efficient electrocatalyst for oxygen evolution reaction. Journal of Colloid and Interface Science, 2020, 574:241-250.
[120] Zheng J, Chen X, Zhong X, et al. Hierarchical porous NC@ CuCo nitride nanosheet networks: Highly efficient bifunctional electrocatalyst for overall water splitting and selective electrooxidation of benzyl alcohol. Advanced Functional Materials, 2017, 27(46): 1704169.
[121] Wang Y, Xie C, Liu D, et al. Nanoparticle-stacked porous nickel-iron nitride nanosheet: A highly efficient bifunctional electrocatalyst for overall water splitting. ACS Applied Materials & Interfaces, 2016, 8(29): 18652-18657.
[122] Yuan H, Wei S, Tang B, et al. Self-supported 3D ultrathin cobalt-nickel-boron nanoflakes as an efficient electrocatalyst for oxygen evolution reaction. ChemSusChem, 2020, 13(14):3662-3670.
[123] Hou L, Shao M, Li J, et al. Two-dimensional ultrathin arrays of CoP: Electronic modulation toward high performance overall water splitting. Nano Energy, 2017, 41:583-590.

用于电催化水分解的三维阵列材料

刘启龙[1], 肖翀[1,2]*
1. 合肥综合性国家科学中心能源研究院,安徽合肥 230031;
2. 合肥微尺度物质科学国家研究中心,安徽合肥 230026
* 通讯作者. E-mail:cxiao@ustc.edu.cn

摘要: 氢能源被认为是最有可能替代化石燃料的清洁能源之一. 探索适用于水分解产氢的催化剂已经成为电解水领域的重要课题. 由于纳米粉体材料导电性不好,且在催化过程中容易堆积,所以将纳米活性物质和导电基底结合起来,构建具有开放多孔结构的三维(3D)阵列电极已经成为电催化领域的研究热点. 本文首先总结了 3D 阵列电极在电催化水分解中的优势,然后介绍了提高材料催化性能的几种策略,最后对用于水分解的阵列催化材料进行了分类和总结,希望能为新的电催化材料的设计和制备提供参考.

关键词: 电催化水分解;氢能源;3D 阵列电极